Effects of Cloud Vertical Structure on Atmospheric Circulation in the GISS GCM

JUNHONG WANG

Program in Atmospheric and Oceanic Sciences, University of Colorado, Boulder, Colorado

WILLIAM B. ROSSOW

NASA/Goddard Institute for Space Studies, New York, New York

(Manuscript received 25 September 1997, in final form 29 January 1998)

ABSTRACT

Thirteen experiments have been performed using the Goddard Institute for Space Studies General Circulation Model (GISS GCM) to investigate the response of the large-scale circulation to different macroscale cloud vertical structures (CVS). The overall effect of clouds, the role of their geographic variations, and difference between the transient and equilibrium responses of the atmospheric circulation are also studied. Clouds act to suppress the Hadley circulation in the transient response, but intensify it in the equilibrium state. Changing CVS affects the atmospheric circulation directly by modifying the radiative cooling profile and atmospheric static stability, but the effect is opposed, on average, by an indirect effect on the latent heating profile produced by deep (moist) convection. Different interactions of radiation and convection with land and ocean surfaces mean that this cancellation of CVS effects on radiative and latent heating is not the same at all locations. All three parameters of the CVS seem equally important: the cloud-top height of the uppermost cloud layer, the presence of multiple layers, and the separation distance between two consecutive layers in a multilayered cloud system. In experiments with a globally uniform, single-layered cloud, the one with the cloud located somewhere at middle levels (720–550 mb in this model) results in the strongest Hadley circulation; with a single-layered cloud located above or below this level, both the circulation intensity and its vertical extent decrease. Inserting another cloud layer below a cloud in the upper troposphere also intensifies the Hadley circulation, the effect increasing with decreasing separation distance. Separately, vertical gradients in the cloud distribution appear to be more important to the circulation strength than horizontal gradients, but horizontal variations in the CVS are needed to explain the strength of the mean circulation in the model atmosphere. The results also suggest that explicitly resolving cloud-top radiative cooling and base warming for each cloud layer is important to modeling the Hadley circulation.

1. Introduction

Much emphasis in recent studies of the role of clouds in the climate is on the average cloud effects on the earth and surface radiation budgets (ERB and SRB) (see reviews by Arking 1991; Wielicki et al. 1995). However, the impact of clouds on the mean ERB and SRB only indicates their influence on the climate indirectly because their direct effects on the atmospheric circulation work through their perturbations of the temporal, vertical, and horizontal distributions of radiative energy *within* the atmosphere (Webster and Stephens 1984).

Satellite observations of cloud-induced changes of ERB constrain the total heat transport by the ocean–atmosphere system (Sohn and Smith 1992a, 1992b, 1992c), but do not provide direct measurements of cloud-induced changes of radiative fluxes at the surface and within the atmosphere. Rossow and Lacis (1990) and Zhang et al. (1995) developed an approach to calculate radiative fluxes at the top-of-atmosphere (TOA) and at the surface by using a radiative transfer model and the physical properties of the clouds, atmosphere, and surface derived from satellite observations. Based on the difference between the net radiative fluxes at TOA and surface, which gives the total net radiative flux into the atmosphere and cloud-induced changes in this difference, Rossow and Zhang (1995) suggested that clouds enhance the latitudinal gradient in the radiative cooling in the atmosphere and, therefore, reinforce the radiative forcing for the mean atmospheric circulation. Zhang and Rossow (1997) extended this study to show that clouds increase the mean meridional energy transport required of the atmosphere and decrease that required of the oceans. Neither of these studies considered the vertical distribution of radiative heating within the atmosphere because their calculations assumed single-layer clouds at each location and time. In addition, how the atmospheric circulation responds to

Corresponding author address: Dr. Junhong Wang, Department of Engineering Sciences, University of Colorado, Campus Box 429, Boulder, CO 80309-0429.
E-mail: jhw@monsoon.colorado.edu

cloud-generated perturbations in the radiation field is beyond the reach of these studies. Using a general circulation model (GCM), we begin to investigate how cloud-induced perturbations of the vertical profile of radiative heating/cooling modify the atmospheric circulation, including feedbacks by moist convection.

B. G. Hunt (1978) found that complete removal of clouds from his model produced surprisingly small changes of the general circulation. This result was criticized as misleading because of the neglect of important feedback mechanisms, such as relative humidity and sea ice albedo feedback (G. E. Hunt et al. 1980); but the insensitivity of the modeled atmospheric circulation to the removal of clouds is most likely due to the fixed sea surface temperature (SST). Meleshko and Wetherald (1981) and Shukla and Sud (1981) investigated the effects of geographic and temporal variations of cloud cover on atmospheric circulations, respectively. Slingo and Slingo (1988, 1991) and Randall et al. (1989) examined the importance to the general circulation of cloud-induced alterations of the longwave (LW) radiative cooling of the atmosphere. Ramaswamy and Ramanathan (1989) also showed that solar heating rates within extensive tropical convective anvil decks ($\sim$1.5 K day^{-1}) influence the atmospheric circulation by regulating the meridional heating gradients within the upper troposphere. Liang and Wang (1997) found that a ''mosaic'' treatment of cloud overlap in a GCM, instead of the commonly used ''random'' overlap scheme, can improve the GCM-simulated climate significantly because of different atmospheric radiative heating/cooling distributions (see also Stubenrauch et al. 1997). These studies are limited because they consider only one part of the cloud effects on the atmospheric circulation and use specified SSTs. In particular, none of these studies investigated the effects of cloud vertical structure on atmospheric circulations, including the effects of variations of cloud top and base heights, cloud-layer thicknesses, and the vertical distribution of multilayered clouds.

Cloud vertical structure (CVS) affects the atmospheric circulation by determining the vertical gradients of radiative heating/cooling and latent heating (e.g., Webster and Stephens 1984). Tropical studies have shown that the extensive tropical cloud clusters associated with cumulus towers can generate notable perturbations of the local radiative heating profile (several tens of kelvins per day) (Webster and Stephens 1980) that are about the same magnitude as those produced by latent heat release and sufficient to alter both the large-scale circulation and deep cumulus convection (Houze 1982; Hartmann et al. 1984; Machado and Rossow 1993). Randall et al. (1989) found that different cloud vertical distributions in two models contributed to the difference in responses of atmospheric circulations to cloud LW radiative forcing in the atmosphere, although the two models have the same vertically integrated ''cloud radiative forcing.'' Slingo and Slingo (1991) found that changing the cloud prediction scheme in their model caused alterations in the vertical profile of ''cloud longwave atmospheric forcing,'' leading to a substantial reduction in surface evaporation and intensification of the twin anticyclones to the north and south of the major tropical diabatic heating anomalies.

Cloud-induced radiative perturbations in a GCM and the GCM-predicted cloud vertical structure cannot be validated because there is little information on CVS available (Wang and Rossow 1995; Wang 1997). Nevertheless, a GCM can be used to study the processes linking CVS to the model circulation and to suggest observational studies to test the validity of these models processes. Such studies might also help define the required observational accuracy for CVS and suggest cloud improvements in GCMs.

It is clear from the above summary of previous studies that CVS is important, but that this importance has not really been quantified nor studied in all respects. In particular, we wish to determine whether the occurrence of multilayered clouds has any significant consequences beyond what can be represented with single-layered clouds. In this study, we performed a series of experiments using a recent version of the NASA Goddard Institute for Space Studies (GISS) GCM to study the effects of CVS on atmospheric circulations. In two ways, our study is unique and different from other studies. First, most other studies examined the effects of removing clouds or varying their heights; we focus on the importance of the vertical structure by exploring quantitatively the different effects between single and multilayered clouds and among multilayered clouds. Second, to understand how CVS influences the circulation, we focus on its role in indirectly modulating latent heating by coupling its direct radiative effect with the convective process in contrast to concentrating on purely cloud-radiative effects as in previous studies.

Thirteen experiments have been conducted using the GISS GCM to study effects of CVS on atmospheric circulations (described in section 2). We focus on the Hadley circulation since changes in the vertical distribution of the total diabatic heating are expected to influence it most directly (Rind and Rossow 1984). In addition, we consider the overall effect of clouds by contrasting the atmospheric circulations with and without clouds and with and without geographic variations of clouds with the circulations obtained with different CVS. We also compare the transient and equilibrium responses of the atmospheric circulation to changed CVS. Since CVS is specified in our experiments, the full feedback among clouds, radiation, and circulation is not allowed. Thus, we focus on the transient experiments, where little change in surface (ocean) temperature has occurred, to isolate the initial tendencies of the circulation changes that should be more representative of the interactions between CVS and the circulation in the model's climate (section 3). In section 4, we explain how the cloud-induced radiative heating

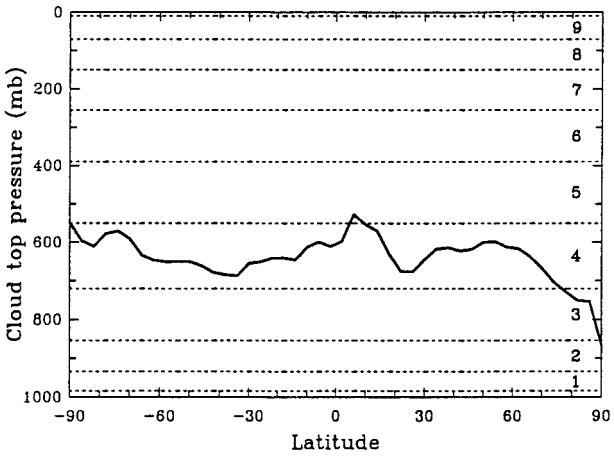

FIG. 1. Zonal mean cloud-top pressure (mb) in January in the control run. Dashed lines represent the boundaries of GCM vertical layers. The numbers denote the layer number.

changes interact with changes in the latent heating by convection to alter the Hadley circulation. Finally, in section 5, several points arising from these experiments are highlighted and discussed.

2. Model and experiments

a. Model description

The general circulation model used in this study is an updated version of Model II developed at GISS (Hansen et al. 1983). The cloud parameterization differs from Model II and is composed of a prognostic cloud water scheme for large-scale clouds (Del Genio et al. 1996) and an improved parameterization of moist convection (Del Genio and Yao 1993). When coupled to a mixed layer (so-called Q-flux) ocean, this model is being used by Yao and Del Genio (1997, personal communication) to study cloud feedbacks on climate simulations. The control run described below is also used in their study. This model has nine vertical layers up to 10 mb (Fig. 1) and a horizontal resolution of $4^\circ \times 5^\circ$ (lat $\times$ long).

Ocean surface temperature and ice cover in the model are computed based on energy exchanges with the atmosphere and specified, geographically and seasonally varying ocean heat capacity (mixed layer depth) and heat transports (Hansen et al. 1984; Hansen et al. 1988). Monthly ocean mixed layer depths are compiled from the National Oceanographic Data Center (NODC) mechanical bathythermograph data (NOAA 1974) and from temperature and salinity profiles in the southern ocean (Gordon 1982); but a 250-m maximum is imposed to reduce computer time. The horizontal ocean heat transport is identical to that in the control run in all experiments; that is, there is no feedback of ocean heat transport on the changing climate.

b. Experiment design

The control run is a 40-yr simulation (started from another model run, so the control run does not represent a particular time period). Thirteen experiments have been performed, categorized into five groups (Table 1), by specifying different *fixed* cloud vertical structures in the radiation model. In Table 1, abbreviations indicate what clouds are specified in the radiation scheme: CLR means clear sky, that is, no clouds are specified, and SL and DL mean that only single-layered and double-layered clouds are specified, respectively. The model layer containing a cloud is indicated by a number (layer 7 is the top of the troposphere and layer 1 is at the surface, see Fig. 1). All experiments, except CLR-E and SL7-E in group 5, were run for three months (December, January, and February) starting on 1 December; the quantities shown have been averaged over these three months. The SL7-E was run for 30 yr, attaining approximate equilibrium after 20 yr. The CLR-E did not quite reach thermal equilibrium, even after a 40-yr run; however, the dynamic quantities (e.g., total angular momentum, wind speeds) appeared to be in equilibrium after 25 yr. The equivalent quantities from the control run and the two equilibrium runs (denoted by E) are averaged over the Januarys in the last 10 yr. The results

TABLE 1. Description of experiments.

Group	Experiment	Experiment description
	Control	The mean of last 10-yr Jan control run
1) Overall cloud's impact	CLR	Clouds removed in the radiation scheme
2) Impact of cloud's latitudinal and longitudinal variations	ZMSL	Zonal mean single-layered cloud
	GDSL	Single-layered clouds with geographic distributions
3) Single-layered clouds	SL3	A single-layered cloud in layer 3
	SL4	A single-layered cloud in layer 4
	SL5	A single-layered cloud in layer 5
	SL7	A single-layered cloud in layer 7
4) Double-layered clouds	DL35	Two-layered clouds in layers 3 and 5
	DL37	Two-layered clouds in layers 3 and 7
	DL57	Two-layered clouds in layers 5 and 7
	DL67	Two-layered clouds in layers 6 and 7
5) Two equilibrium runs	CLR-E	CLR with 40-yr running period
	SL7-E	SL7 with 30-yr running period

from all experiments, except the control run, CLR-E and SL7-E, represent initial tendencies before the ocean temperature has changed significantly rather equilibrium changes where additional feedbacks come into play.

Many studies of cloud-radiative effects have been done by changing the geographic or temporal variations of clouds or removing part of their radiative effects (e.g., Meleshko and Wetherald 1981; Shukla and Sud 1981; Le Treut and Laval 1984; Slingo and Slingo 1988, 1991; Randall et al. 1989). However, only B. G. Hunt's simulations provided a very unique understanding of the total cloud effect by completely removing the clouds. Given all the changes in GCMs made in the past 18 yr, repeating this experiment can provide an interesting assessment of the role of clouds in current models for comparison with the effects on atmospheric circulations implied by satellite observations and radiative transfer calculations (Sohn and Smith 1992a; Rossow and Zhang 1995). In CLR and CLR-E (Table 1), all clouds are removed in the radiation scheme at each radiation time step (5 h). We compare the transient and equilibrium responses of the atmospheric dynamics to cloud-radiative effects using CLR and CLR-E.

In the other 11 experiments, the radiative effects of CVS on the model circulation are isolated by preserving the total column cloud cover, optical thickness, and particle size that are predicted by the cloud subroutines at each time step, but rearranging the CVS to a prespecified arrangement in the radiation subroutine (cloud phase can change with temperature if the cloud is moved from its predicted location). This approach preserves the total solar heating, most of which occurs at the surface, and emphasizes changes in the vertical distribution of longwave cooling of the atmosphere. Since CVS is fixed in each experiment at each time step, there is no feedback on CVS when the atmospheric circulation changes; however, there are feedbacks on cloud cover, optical thickness, and particle size (that turn out to be negligible in the transient experiments).

Clouds also vary geographically, and such variations can also play an important role in modulating atmospheric circulations (cf. Meleshko and Wetherald 1981). To isolate variations in CVS from geographic variations, we ran two experiments with zonal mean and geographically varying single-layer clouds (ZMSL and GDSL in group 2 in Table 1), respectively, to study the effects of the latitudinal and longitudinal cloud variations on the mean meridional circulation (MMC). The single cloud layer in these experiments is in the average location of the clouds in the control run (layer 4 in the zonal mean for most latitudes, see Fig. 1).

Experiments in groups 3 and 4 (Table 1) focus on the impacts of CVS by assuming a *globally uniform CVS.* The global mean cloud layer location in the control run is in layer 4 (720–550 mb). In SL4, a single-model-layer cloud is specified in layer 4 at all cloudy locations at each time step with the same predicted total column optical depth and total cloud cover. The global mean frequency of multilayered clouds (defined as cloud layers with at least one intervening clear layer) in the control run is 23.5% with an inhomogeneous geographic distribution (not shown). Surface observations indicate multilayered cloudiness about 49% of the time, and rawinsonde humidity profiles imply the occurrence of multilayered clouds about 46% of the time (Wang 1997). Thus, the model underestimates the frequency of multilayered clouds probably because of its coarse vertical resolution. Most of individual cloud layers (76.5% globally) are only one model-layer thick. Therefore, we also compare to the control run an experiment (DL35), where we specify cloud layers in layer 3 and layer 5, globally, to give the same global mean location as the control run. The total column optical depth is distributed in two model layers in proportion to their physical thicknesses. The control run CVS is thus intermediate between the extremes of SL4 and DL35. In the remaining experiments in groups 3 and 4, other single- and double-layer CVS are specified. The SL7-E is the same as SL7, except that it has been run to equilibrium.

3. Effects of CVS changes on MMC

The zonally averaged mass stream function and its standard deviation for the last 10 Januarys in the control run are shown in Fig. 2. The Hadley cell is more intense in the Northern Hemisphere (NH). The distribution of standard deviations (Fig. 2b) indicates that larger year-to-year fluctuations occur in the ascending branches of the Hadley cells in both hemispheres and in the center of Ferrel cell in the NH. In the discussion of the experiments, only changes in the mean circulation that exceed the standard deviation in the control run are considered to be significant. The simulated Hadley cell in our model (Fig. 2a) is 10%–20% too weak and extends several degrees too far north in comparison to observations (Hansen et al. 1983; Rind and Rossow 1984). These deficiencies may distort the results of our simulations; we note that Rind and Rossow (1984) show that their results from even more extreme changes were of a similar nature using two different versions of the GISS model. We focus our attention on the Hadley circulation because changes in the diabatic heating have a more direct effect on it (Rind and Rossow 1984), but some variations in the Ferrel cells are briefly discussed. In this section we will describe only the changes in the MMC that occur in the experiments and hold explanations until section 4.

a. Vertically integrated MMC

Table 2 summarizes the characteristics of the zonal mean, vertically integrated Hadley and Ferrel circulations for the control run and all of the experiments. The latitudinal limits of the Hadley cells are determined by the latitudes where the vertically integrated stream function is negative for NH and positive for the Southern

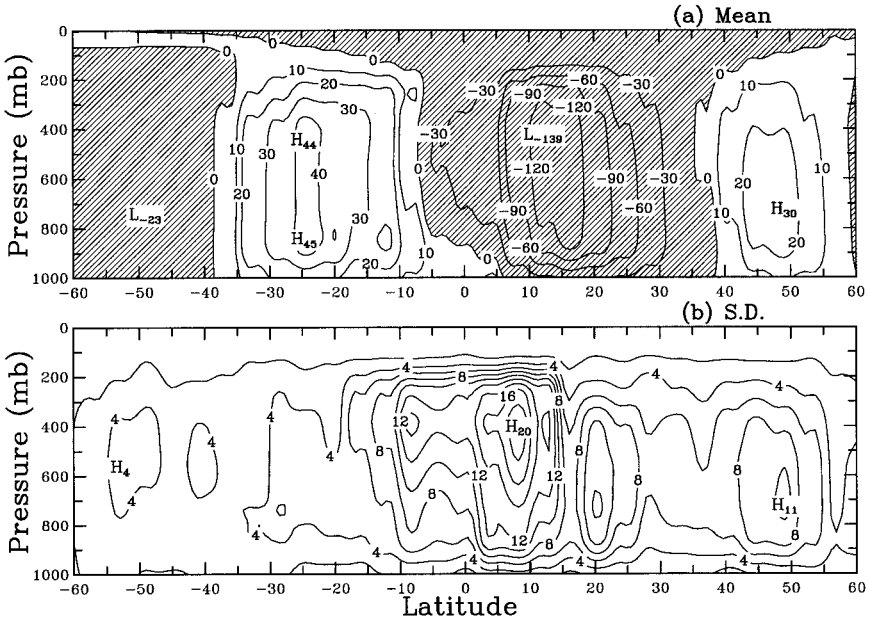

FIG. 2. (a) Zonal mean mass stream function and (b) its standard deviation (10^9 kg s^{-1}) in January for the mean of 10-yr control run.

Hemisphere (SH). The latitudinal gradient of the vertically integrated diabatic heating, $\partial H/\partial y$, is the primary drive for the Hadley circulation (Rind and Rossow 1984) and is calculated at latitudes of peak stream function intensity. Total diabatic heating is the sum of radiation cooling, moist and dry convective heating, and latent heating by precipitation in large-scale clouds.

Table 2 shows that the peak intensities of the NH Hadley cell are decreased in all experiments compared with the control run, which is directly associated with reduced latitudinal gradients of the diabatic heating. The correlation coefficients between the peak intensity and $\partial H/\partial y$ in the Northern and Southern Hemisphere are 0.80 and 0.62, respectively. The eddy contributions to the MMC forcing, both the eddy heat and momentum fluxes, are responsible for a thermally indirect Ferrel cell in the extratropics. In all experiments, the Ferrel cells in both hemispheres are weaker than in the control run because of decreased eddy kinetic energy (Table 2).

The equatorward limit on the Hadley circulation is set by the location of the maximum total heat source (Rind and Rossow 1984), which is approximately constant in all the experiments (not shown). The only significant latitude shifts of the equatorward limit of the

TABLE 2. Zonal mean vertically integrated general circulation characteristics.

	Hadley cell (Northern–Southern Hemispheres)					Ferrel cells (Northern–Southern Hemispheres)		
Experiment	Peak intensity (10^9 k gs^{-1})	Peak latitude	N limit	S limit	$\delta H/\delta y$ (10^7 W m^{-1})	Peak intensity (10^9 kg s^{-1})	Peak latitude	EKE (10^4 J m^{-2}) (36°N,52°S)
Control	−94.7/29.4	16°N/24°S	38°N/ 6°S	6°S/38°S	4.27/1.63	16.0/−15.1	48°N/48°S	188.1/122.1
CLR	−89.9/30.6	12°N/24°S	38°N/10°S	10°S/38°S	3.15/2.88	15.3/−12.9	48°N/48°S	165.6/120.5
ZMSL	−91.6/34.6	16°N/12°S	38°N/ 6°S	6°S/34°S	3.32/4.96	13.3/−11.0	48°N/44°S	183.6/113.0
GDSL	−90.4/31.1	16°N/24°S	38°N/ 6°S	6°S/38°S	3.91/1.62	13.3/−13.1	48°N/44°S	169.2/117.6
SL3	−82.2/29.3	16°N/24°S	38°N/ 6°S	6°S/34°S	2.94/1.68	13.3/−13.0	44°N/48°S	183.1/105.9
SL4	−87.0/31.0	16°N/24°S	38°N/ 6°S	6°S/38°S	3.91/1.41	16.3/−13.3	48°N/48°S	174.1/121.1
SL5	−82.8/30.0	16°N/24°S	38°N/ 6°S	6°S/38°S	2.94/2.11	7.7/−15.6	48°N/48°S	170.2/120.5
SL7	−54.7/15.1	16°N/24°S	46°N/10°S	10°S/38°S	2.30/1.30	5.9/ −6.9	56°N/52°S	99.8/ 69.5
DL35	−86.5/32.0	16°N/24°S	38°N/ 6°S	6°S/34°S	2.96/2.06	13.0/−13.6	48°N/48°S	180.8/121.6
DL37	−64.4/15.9	16°N/20°S	40°N/10°S	10°S/38°S	2.35/0.62	8.2/ −9.2	48°N/48°S	123.2/ 75.6
DL57	−72.6/21.6	16°N/24°S	42°N/10°S	10°S/38°S	2.59/2.13	11.8/−11.1	52°N/48°S	131.6/ 83.5
DL67	−81.3/17.7	12°N/24°S	40°N/10°S	10°S/38°S	1.99/1.72	10.0/ −6.3	48°N/52°S	123.3/ 63.4
CLR-E	−51.8/26.9	28°N/32°S	60°N/14°S	14°S/45°S	0.95/1.16	*	*	42.6/ 29.3
SL7-E	−65.2/13.3	16°N/32°S	56°N/18°S	18°S/58°S	2.94/0.54	*	*	67.2/ 31.7

* Ferrel cells disappear.

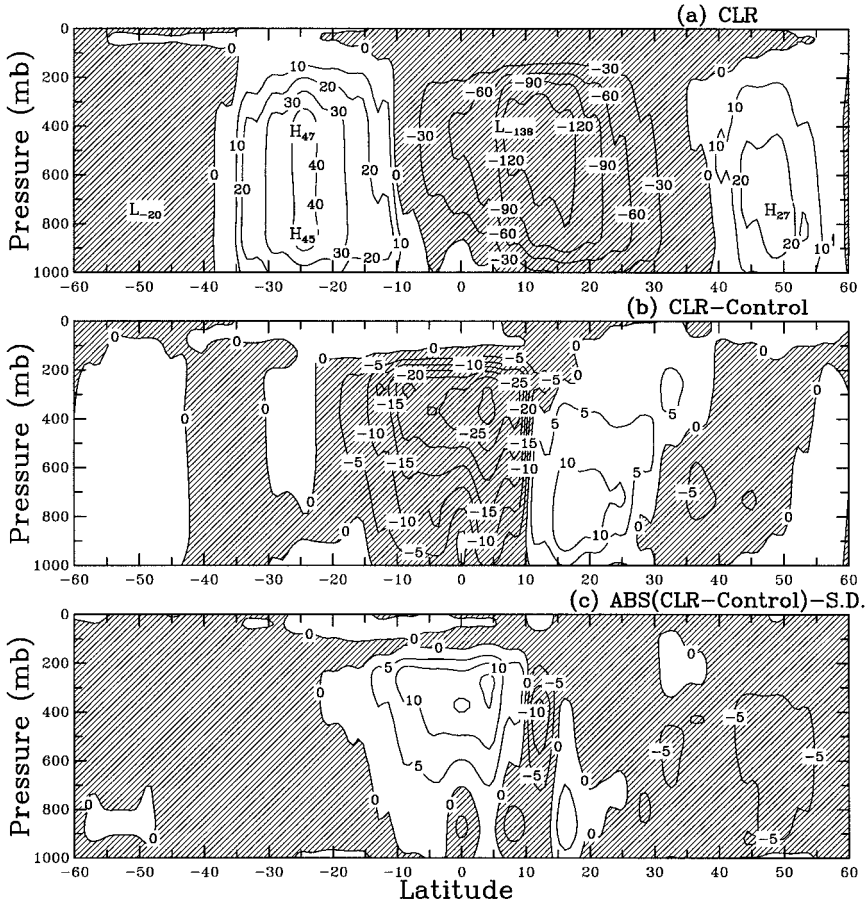

FIG. 3. (a) Zonal mean mass stream function (10^9 kg s^{-1}) for the clear sky in the transient run (CLR), (b) the difference in stream function between CLR and the control run, (c) the difference between the absolute values of (b) and the standard deviation of stream function in the control run.

Hadley circulation occur in the two equilibrium experiments (CLR-E and SL7-E), where there is a southward shift of Hadley cell in the NH (discussed in section 4). Rind and Rossow (1984) concluded that the location of the polarward limit of the Hadley cell depends on the relative intensities of the forcing for the Hadley and Ferrel cells. Both Hadley and Ferrel cells in the NH are weakened in all experiments, so that the poleward limit remains about the same (poleward shifts $\leq 4°$ lat, the horizontal resolution of the model), except in SL7 and the two equilibrium experiments. In SL7, the 63% decrease in the peak intensity of the Ferrel cell in the NH exceeds the 42% decrease of the Hadley cell, leading to an 8° poleward shift of the dividing line between the Hadley and Ferrel cells. In the two equilibrium experiments, the Ferrel cells disappear and the Hadley cells extend to the poles.

b. Overall impact of clouds

In the cloud-free transient run (CLR), the ascending branch of the NH Hadley circulation intensifies and spreads southward and upward compared with the control run (Fig. 3). This initial tendency of removing clouds to enhance the Hadley circulation appears to contradict the conclusion from satellite analyses of cloud effects on the radiative forcing for the MMC (Sohn and Smith 1992a; Rossow and Zhang 1995). However, as explained in section 4b, this disagreement disappears when the results of the equilibrium experiment (CLR-E) are examined: Figure 4 shows that, with all clouds removed, the Hadley circulations in both hemispheres, especially the NH, are much weaker (only 48% of peak intensity in the NH) than in the control run; but extend over a wider range of latitudes and to larger heights (Figs. 2a and 4a). In other words, in the equilibrium state, clouds serve to intensify the Hadley circulation intensity, but reduce its latitudinal and vertical extents. A similar result appears in the other equilibrium experiment (SL7-E) (see Fig. 9a). In these equilibrium states, atmospheric conditions and, consequently, some of the cloud radiative effects are substantially different from the control run. For instance, global mean surface temperature has increased to 27°C and 42°C in SL7-E

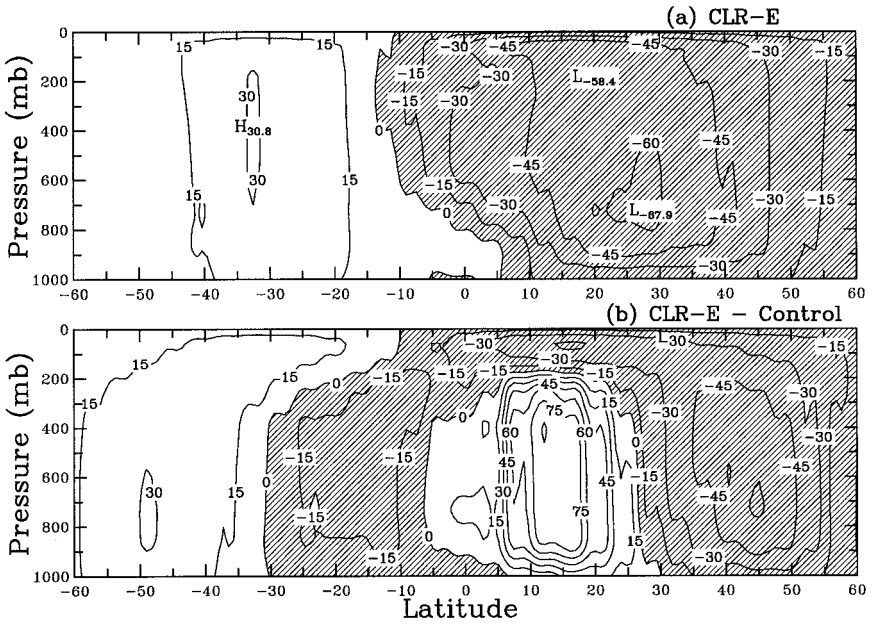

FIG. 4. (a) Zonal mean mass stream function (10^9 kg s^{-1}) for the clear sky in the equilibrium run (CLR-E) and (b) the difference between CLR-E and the control run.

and CLR-E, respectively, from 3.5°C in the control run. To isolate the direct effects of CVS without the additional feedbacks that come into play when atmospheric properties are significantly altered, we focus on the transient responses of the model in this study.

c. Impact of latitudinal and longitudinal cloud variations

In the ZMSL experiment, a single-layered cloud is placed at the zonal mean height of the control run clouds and in the SL4 experiment, a globally uniform, single-layered cloud is specified in layer 4, the global mean height of the control run clouds. Comparing the mean stream functions in these two experiments illustrates the influence of latitudinal variations of CVS in the model (actually it is the variations of cloud-top height because only single-layered clouds are used). The results (Fig. 5a) indicate that the meridional variations of CVS tend to amplify the Hadley circulations in both hemispheres. In the GDSL experiment, the longitudinal variations of the cloud-top heights of a single-layered cloud are added to the ZMSL distribution. The differences between GDSL and ZMSL in Fig. 5b show that the longitudinal variations of CVS diminish the Hadley circulations in both hemispheres. Thus, the latitudinal and longitudinal variations of CVS have opposite effects on the Hadley circulations. Note that only magnitudes of differences in stream function in 20°–10°S in Figs. 5a,b are larger than the standard deviations in the control run.

Since the effects of the latitudinal and longitudinal CVS variations oppose each other and since testing the effects of CVS on the circulation is more complicated if geographic variations must also be specified, we have simplified the experiments by using a globally uniform CVS. Thus, the tendency of changes in CVS in the remaining experiments is judged by comparison with the SL4 experiment, where a single-layered cloud is located at the global mean cloud location of the control run clouds.

d. Impact of CVS changes

The differences between a single-layered cloud and double-layered clouds, both with the same global average height as in the control run (layer 4), are illustrated by comparing experiments SL4 and DL35 (Fig. 6). Both exhibit similar Hadley circulations in the SH as in the control run; but the NH Hadley circulation in DL35 is stronger, in better agreement with the control run, because it better approximates the higher frequency of multilayered cloudiness in the NH in the control run. The weaker NH Hadley circulation in SL4 compared with the control run arises despite some enhancement of the descending branch.

The vertically integrated peak intensities of the NH Hadley circulation in experiments with a single-layer cloud above layer 4 (SL5 and SL7) or below layer 4 (SL3) are smaller than with a cloud in layer 4 (SL4) (Table 2). In other words, the initial effect of the radiative perturbation caused by placing a single cloud layer somewhere near the middle of the troposphere produces the strongest Hadley circulation. Moving the cloud layer either up (SL5 and SL7) or down (SL3) from layer 4 suppresses the descending branch of the Hadley cell in the NH, the effect becoming stronger and

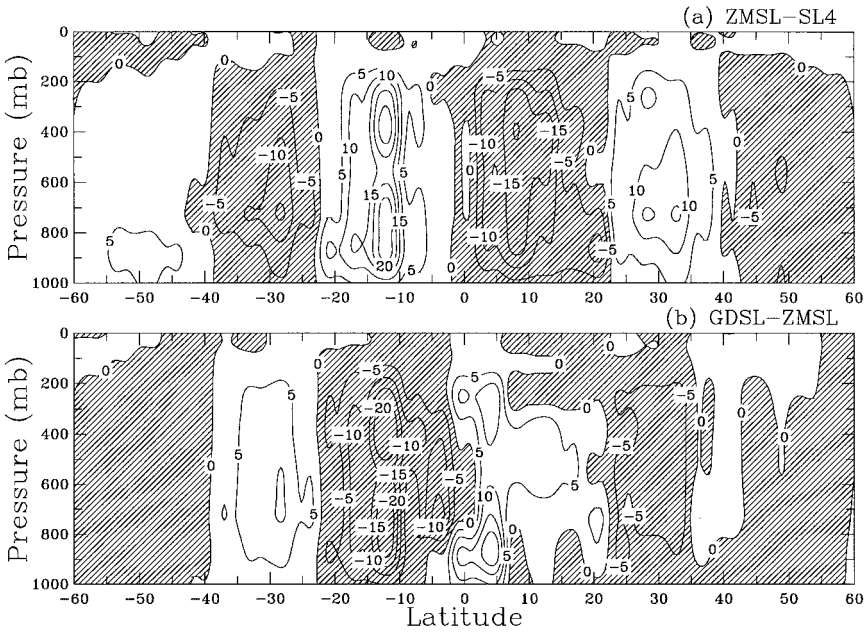

FIG. 5. The difference in zonal mean stream function (10^9 kg s^{-1}) (a) between ZMSL and SL4 and (b) between GDSL and ZMSL.

extending farther toward the center of the ascending branch as the cloud layer moves farther from layer 4 (Fig. 7). This weakening of Hadley circulation is offset by an intensification of the ascending branch of the NH Hadley cell by a cloud in layer 5 (Fig. 7b). When the cloud is in the upper troposphere (layer 7), the SH Hadley cell is significantly weakened compared with SL4 (Fig. 7c) and the locations of the maximum stream function of both Hadley cells move down from around 500 mb in SL3, SL4, and SL5 to around 800 mb.

For two-layered clouds with the same lower-layer location in layer 3 (DL35 and DL37), the experiment with the higher cloud-top height (DL37) produces a weaker but wider Hadley circulation in both hemispheres (Table 2) with a lower altitude of the peak stream function. For two-layered clouds with the same upper-layer location

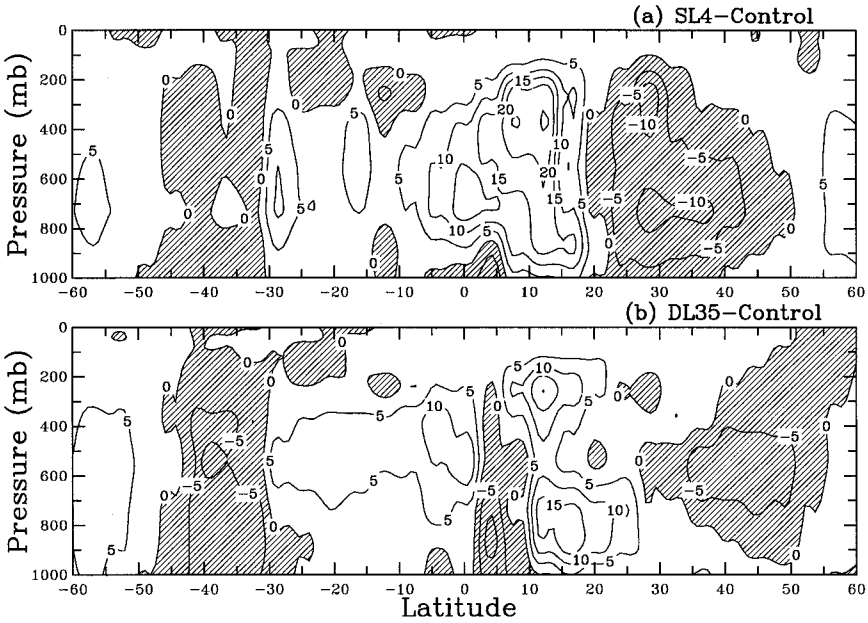

FIG. 6. The difference in zonal mean stream function (10^9 kg s^{-1}) (a) between SL4 and the control run, and (b) between DL35 and the control run.

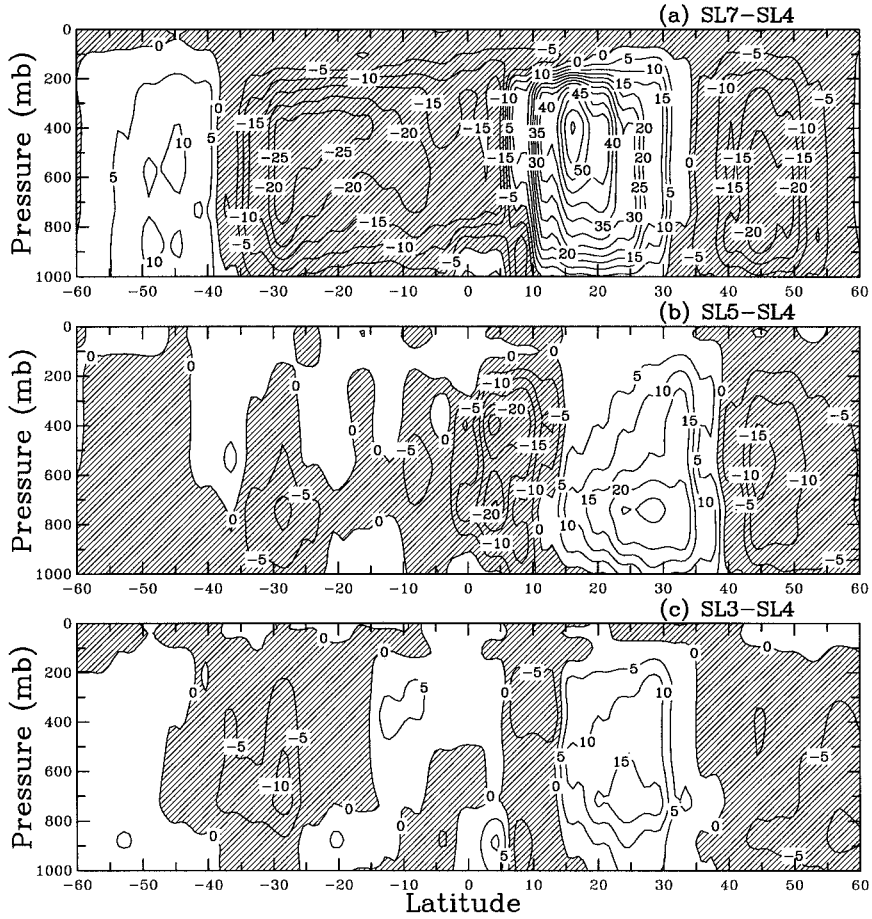

FIG. 7. The difference in zonal mean stream function (10^9 kg s^{-1}) between the cases with a single-layer cloud in layers (a) 7, (b) 5 and (c) 3 and the case with a cloud in layer 4.

in layer 7 (DL37, DL57, and DL67), the Hadley circulation is stronger relative to the experiment (SL7) with a single-model-layer cloud in layer 7, particularly in the NH (Fig. 8). As the altitude of the lower layer increases, both the magnitude of the intensification and the altitude of the peak stream function increase (Fig. 8). The maximum magnitude of the stream function is 104, 105, and 145 $\times$ 10^{-9} kg s^{-1} and the pressure of the peak is at 800, 400, and 250 mb for DL37, DL57, and DL67, respectively. The experiments SL7 and DL67 have the same cloud-top pressure but different cloud vertical extents and generate very different general circulations (Fig. 8a), indicating the importance of cloud-layer thickness and GCM vertical resolution to the resulting circulation (see section 4e).

SL7-E has the same CVS as SL7, but illustrates the circulation attained in equilibrium. Figure 9 shows that the NH Hadley circulation is weaker in the equilibrium than the transient circulation, while there are local intensifications and a larger latitudinal extent in the upper troposphere. This shows that the additional feedbacks that occur once the ocean and atmospheric temperatures begin to change can alter the total effect of CVS on the atmospheric circulation (cf. section 3b).

4. Explanations on changes of MMC

In this section, we present an explanation of how, in our model, changes in CVS produce the Hadley circulation changes described in section 3 by modifying the radiative cooling and, indirectly, the latent heating. Since the changes of MMC presented, especially involving feedbacks, may be particular to the GISS GCM, the explanation is model dependent. This model dependence will be discussed further in section 5. Nevertheless, the model explanation is also a plausible theory of how the real atmospheric circulation might respond to changes in the CVS.

a. Basic theory

Rind and Rossow (1984) illustrated the influences of different heat, momentum, and moisture budget processes on the mean meridional circulation (MMC). The

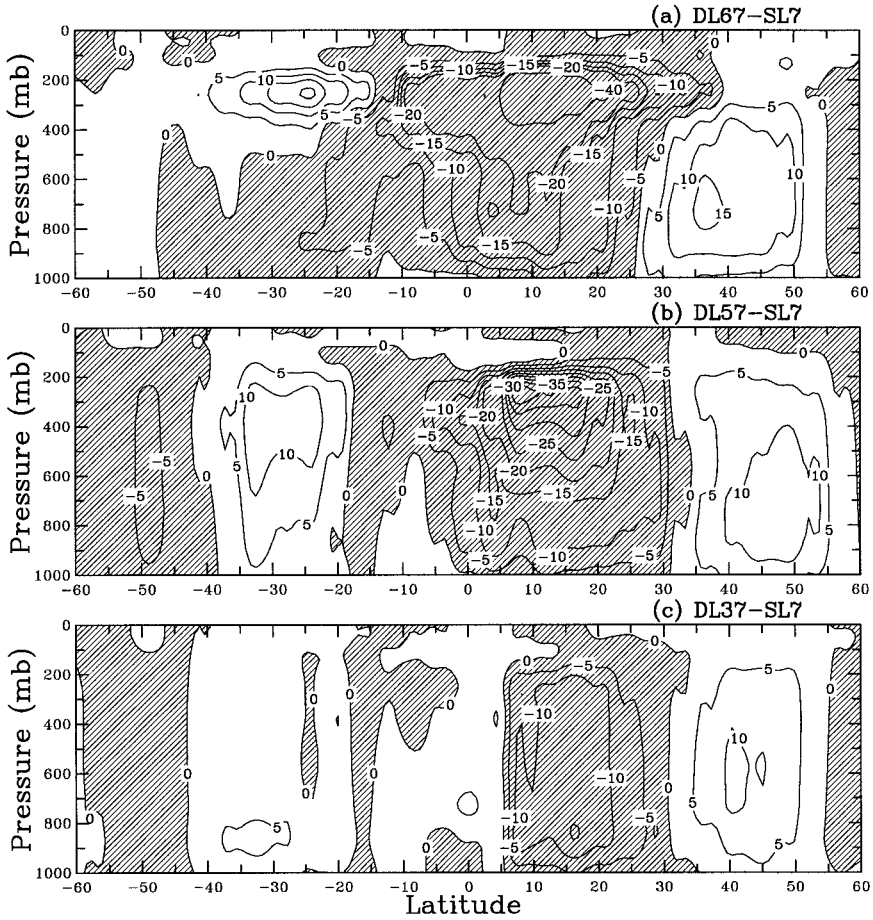

FIG. 8. The difference in zonal mean stream function (10^9 kg s^{-1}) between the experiments with two-layered clouds in layers (a) 7/6, (b) 7/5, and (c) 7/3 and the experiment with a single-model-layer cloud in layer 7 (SL7).

latitudinal gradient of the diabatic heating ($\partial H/\partial y$) is the primary drive for the Hadley circulation; decreasing diabatic heating with latitude forces a thermally direct circulation. The total diabatic heating of the atmosphere, and its two main components, radiative cooling and moist convective heating, in the control run for January are shown in Fig. 10. The maximum heat source is at 6°N, produced mainly by latent heat release in the intertropical convergence zone, while the radiative cooling, which dominates in the subtropics, attains a local minimum there. There is a secondary peak of diabatic heating near 6°S. Overall, $\partial H/\partial y < 0$ (Fig. 10).

In the 13 experiments (Table 1), cloud vertical structures are altered from what the model predicts to the specified CVS in the radiation subroutine. Not only do these changes directly induce perturbations in the radiative heating/cooling rate profiles, which are easily interpreted from the changed cloud distributions, but they also induce changes in the convective latent heating through several feedback relationships. Latent heat release in the Tropics is controlled by atmospheric thermodynamics (dry and moist static stability), the large-scale dynamics (convergence of moist energy), and surface evaporation (cf. Fu et al. 1994). The feedback relationships in the GISS GCM are illustrated in Fig. 11. At each model time step, the four physics subroutines of concern here run in order: large-scale (explicit) dynamics, moist convection, large-scale clouds, and radiation. The key point is that the temperature and humidity fields are updated at the end of each subroutine.

Staring at the end of time step 1, the CVS specified for the particular experiment is inserted into the radiation subroutine, regardless of what vertical distribution was predicted by the previous run. The changed CVS directly alters the radiative cooling, which modifies the atmospheric temperature profile and the moist static stability. At the beginning of time step 2, the large-scale atmospheric dynamics (we focus on the Hadley circulation) reacts to the pressure gradients implied by horizontal and vertical variations of temperature obtained from the aggregated effects of the four subroutines in time step 1. The Hadley circulation then modifies the moist static stability of the atmosphere by transporting heat and water vapor. The subgrid-scale convection then

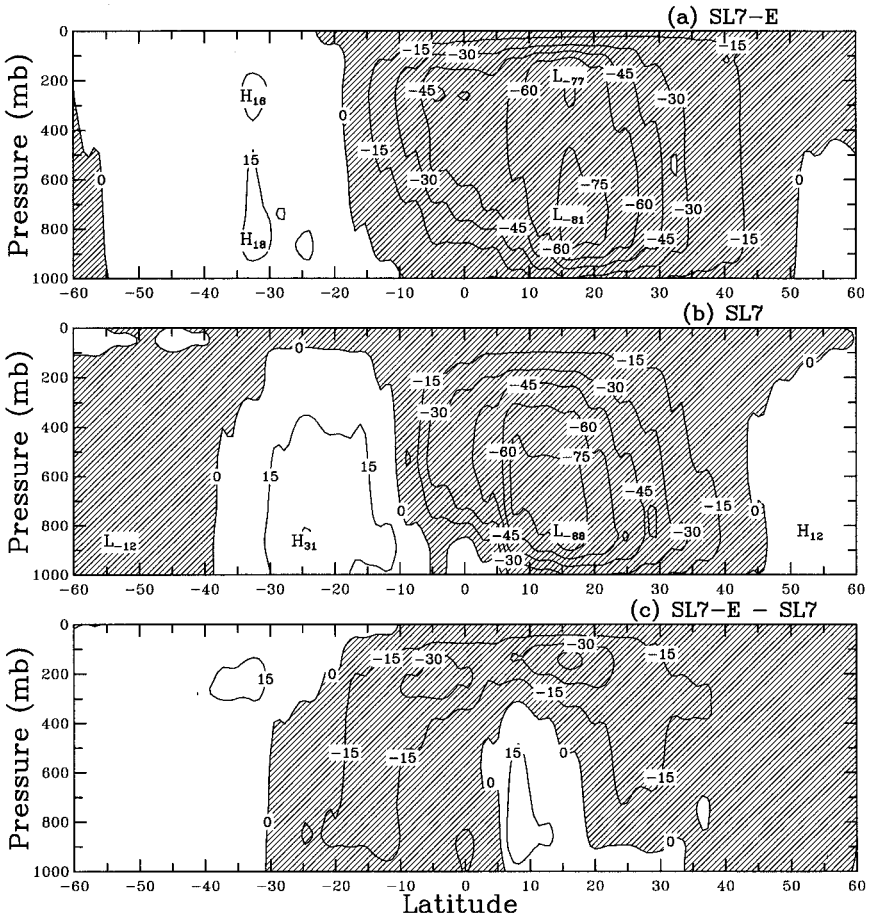

FIG. 9. Zonal mean stream function (10^9 kg s^{-1}) for the experiments with a single-model-layer cloud in layer 7 (a) in the equilibrium state (SL7-E) and (b) the transient state (SL7) and (c) their difference.

reacts to the given large-scale convergence and surface fluxes of heat and water vapor, together with moist static stability. Convective heat and water vapor transports and released latent heating then alter the moist static stability further. The properties and vertical distribution of convective clouds are also predicted. Then the model does the same thing to the large-scale layer clouds. The accumulated vertical distributions of temperature, humidity, and clouds are then passed to the radiation subroutine to end time step 2; however, in our experiments the CVS is again changed to the one specified for that case. The main point illustrated by Fig. 11 is that changes of the cloud vertical distribution perturb the radiative cooling and alter the Hadley circulation; together the radiation and Hadley circulation change the latent heating by convection (and layer clouds) in the Tropics, which produces a feedback on the Hadley circulation. However, radiative cooling dominates in the subtropics (Fig. 10) and so, since Hadley circulation depends on the meridional gradient of diabatic heating, the contrast of opposing diabatic heating changes in the Tropics by radiation and deep convection with that of radiation (almost alone) in the subtropics will alter the Hadley circulation further.

b. Clear versus cloudy skies

The initial tendency caused by removing all the clouds in the GISS GCM is to increase the radiative cooling of the tropical troposphere, but decrease it at higher latitudes (Fig. 12a), consistent with the finding of Rossow and Zhang (1995). Removing clouds in the radiation scheme (dashed line in Fig. 13) also warms the surface in the Tropics. This destabilization encourages the release of more latent heat by convection (Fig. 12b). Note that the increase of vertically integrated latent heating at 6°N (dominated by a precipitation maximum in the western Pacific in January, Fig. 14a) is much smaller than it is near 6°S (dominated by precipitation maxima over South America and Africa, Fig. 14a). Figure 14b also indicates the suppression of the precipitation maxima over the SH tropical land areas by the cloud radiative effects.

The precipitation maxima in the Tropics respond dif-

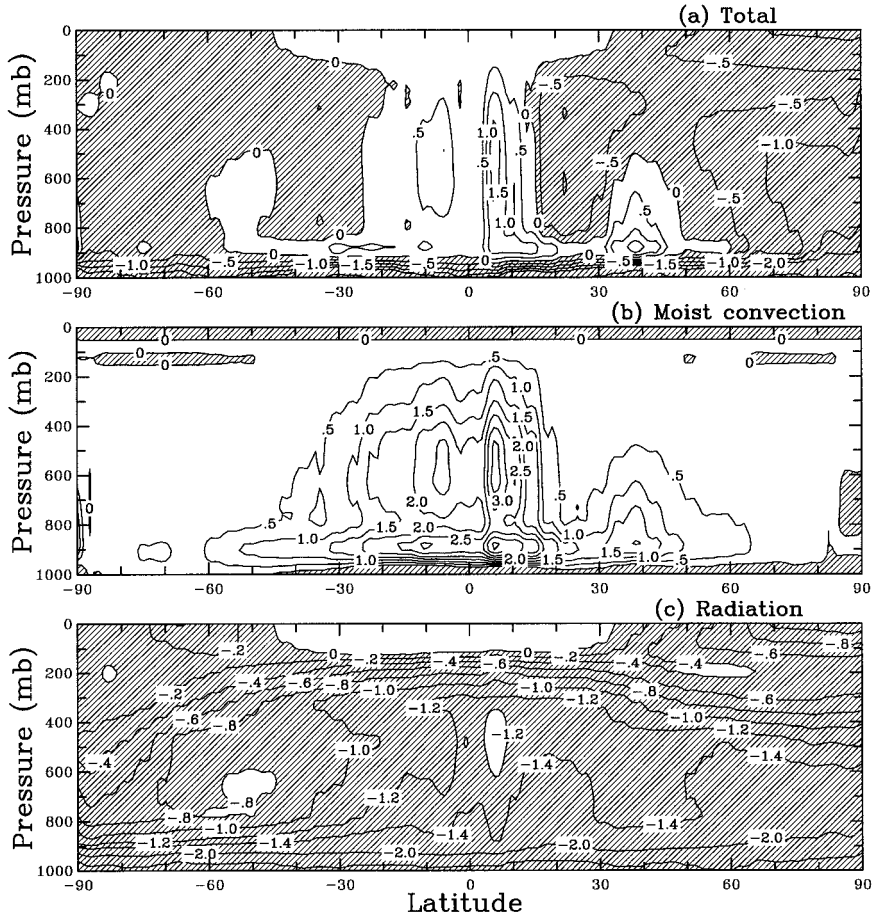

FIG. 10. (a) The total diabatic heating rate in the atmosphere in January in the control run and its two main components, (b) the moist convective heating and (c) radiative heating in units of K day^{-1}.

ferently over land and ocean to the removal of clouds (CLR) or moving all clouds to layer 7 (SL7) (Figs. 14b,c). The largest change occurs over land in CLR (increasing, Fig. 14b), but occurs over ocean in SL7 (decreasing, Fig. 14c). This can be understood from different radiative cooling profiles in CLR and SL7 (Fig. 13) and the slower response of ocean surface temperature to changes in surface radiative heating. In CLR, the transient surface heating shown in Fig. 13 occurs only over land, reinforcing the destabilization of the troposphere by removing clouds, so the precipitation increases over land are larger than over oceans (Fig. 14b). In SL7, however, the radiative heating at the surface is smaller than in the middle and higher troposphere, resulting in a more stable atmosphere compared with the control run (Fig. 13). Without the more rapid surface heating of the land surface, the stabilization is stronger over ocean, leading to a stronger precipitation decrease there (Fig. 14c).

Because of the differing land–ocean responses to removing clouds (a globally uniform change), the resulting changes of latent heating do not compensate the radiative cooling (Figs. 12a,b) the same way everywhere; hence, the secondary peak of total diabatic heating increases and moves 4° southward, while there is little change in the primary peak near 6°N (Fig. 12c). In the subtropics, Fig. 12a shows that there are only minor changes in the radiative cooling (since the clouds originally were mostly low level) that dominates the total diabatic heating there. This combination of changes intensifies the ascending branch of the Hadley cell in the NH and shifts it southward by 4° (Fig. 3 and Table 2). Although the satellite analyses (Sohn and Smith 1992a; Rossow and Zhang 1995) correctly indicate the initial tendency caused by cloud effects on radiation, the actual response of the real atmosphere is likely to be more complicated because of feedbacks by convection (though not necessarily the same as in this model).

The intensification of the Hadley circulation under clear sky has several positive feedbacks on latent heat release in the Tropics; there is more moisture convergence into the Tropics and more surface evaporation under the clear sky (not shown). In this GCM, thermodynamic changes, large-scale dynamics, and surface

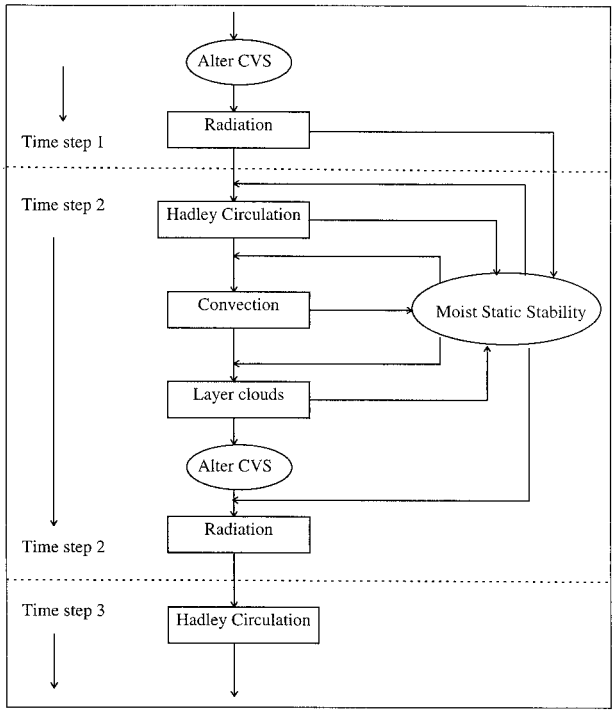

FIG. 11. Schematic showing how perturbations in cloud distributions in the Tropics affect Hadley circulations. See section 4a.

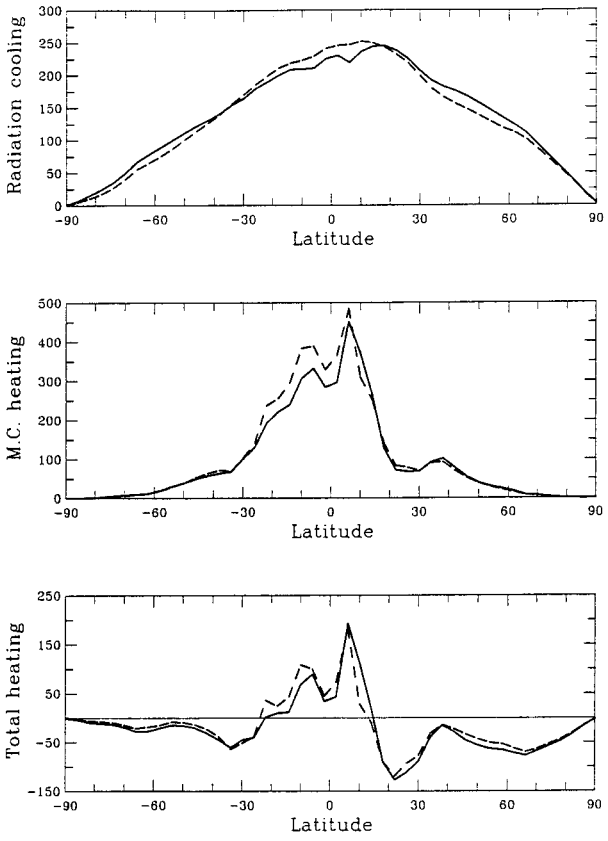

FIG. 12. (a) Vertically integrated radiative cooling, (b) moist convective heating, and (c) total diabatic heating as a function of latitude in the unit of 10^{13} W for the control run (solid line) and CLR (dashed line).

evaporation all lead to more latent heat release when clouds are completely removed.

c. Transient versus equilibrium response

In the two experiments run to equilibrium (CLR-E and SL7-E), the final atmosphere is cooled more by radiation at all latitudes compared with the control run (Fig. 15a) because atmospheric temperatures are higher (see Fig. 16). This differs from the corresponding transient runs (CLR and SL7) (Figs. 12 and 17) where, although the radiation is changed by altering the clouds, the atmospheric and surface temperatures have not yet responded much after three months. In SL7-E, the effects of the atmospheric temperature and humidity increases overwhelm the opposing effect of raising cloud-layer height (see Fig. 16 for SL7-E). Although this result may not be realistic, because we fix the cloud-layer structure regardless of changes in the circulation, it illustrates the complex interplay of the clouds, surface, and atmosphere in determining the radiation balance; it is overly simplistic to consider a simple direct response to a cloud change.

In CLR-E and SL7-E, the tropical atmosphere is heated at the surface and lower levels and cooled at higher levels by radiation (not shown, see Fig. 16 for temperature in SL7-E). As a result of this destabilization, there is more latent heat release (Fig. 15b). The maximum of latent heating moves from 6°N to 6°S (Fig. 15b). Overall, latent heating and radiative cooling still partially compensate each other, producing the two maxima and extending the zone of net diabatic heating to higher latitudes (Fig. 15c). Consequently, the latitudinal gradient of total diabatic heating is actually reduced and the resulting Hadley circulations are weaker in intensity but wider in latitudinal extent (Figs. 4 and 9).

d. Single-layer clouds versus double-layer clouds

Moving a single-layer cloud above (below) the original global mean location (layer 4) produces warming (cooling) by radiation in the atmosphere at all latitudes compared to SL4 (Fig. 17a). Figure 11 shows that moving the cloud layer affects the vertical profile of radiative cooling in the Tropics and, consequently, also leads to changes in latent heat release by convection. Figure 18 shows that, when a single-layer cloud is lifted to layer 7 (dot–dashed line in Fig. 18), the boundary layer cools and the atmosphere above it warms, which produces a 46% increase in static stability and a significant reduction of latent heating (Fig. 17). In the Tropics this decrease in latent heating is partially offset by the decreased radiative cooling caused by the higher clouds, whereas radiative cooling dominates in the subtropics;

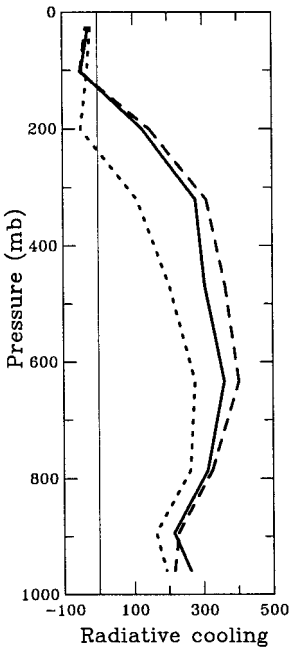

FIG. 13. Vertical profiles of integral of radiative cooling from 15°S to 15°N in the unit of 10^{13} W for the control run (solid line), CLR (dashed line), and SL7 (dotted line).

hence, the latitudinal gradient of total diabatic heating is reduced and the Hadley circulation suppressed (Fig. 17c). Variations in SL5 are similar, though smaller than in SL7; variations in SL3 are similar but opposite in sign.

A global distribution of single-layer clouds is not realistic; the GISS GCM produces multilayered cloudiness about 24% of the time with a distinct geographic pattern, where observations imply a frequency of multilayered clouds that is higher (cf. Warren et al. 1985; Wang and Rossow 1995; Wang 1997; Jin and Rossow 1997). The Group 4 (Table 1) experiments exaggerate the effects of multilayered cloudiness by assuming that all clouds are two layered. The first two cases have the lower cloud in layer 3 but different upper-level cloud locations. The weaker but wider Hadley cells in DL37 than in DL35 described in section 3d can be understood from the explanations for the differences between SL7 and SL5 (cf. Figs. 17 and 18).

The remaining experiments have the upper cloud in layer 7 with a variable lower cloud location. As the separation between the two cloud layers increases, a larger portion of the middle atmosphere within and above the lower cloud layer in the Tropics is cooled by radiation, but the atmosphere below the lower layer is warmed compared with clouds only in layer 7 (the cooling is stronger than heating, Fig. 19). As a result, the vertically integrated radiative cooling increases (not shown). Inserting a cloud layer into layer 6 generates a dipole structure of radiative heating/cooling within the clouds, heating in layer 6 and strong cooling in layer 7 (Fig. 19), also leading to an increase of the vertically integrated radiative cooling (not shown). This vertical structure of the radiative cooling accounts for a reduction of the static stability by two-layered clouds (Fig. 20). The unstable atmosphere releases more latent heat in the Tropics (not shown). The latitudinal gradient of total diabatic heating for two-layered clouds is also increased because the latent heating is partially offset by radiation only in the Tropics, intensifying the Hadley circulation (Fig. 8). Moreover, surface evaporation increases for two-layered clouds because the surface winds are stronger for the stronger circulation, serving as a positive feedback. As the height of the lower cloud layer increases, the atmosphere becomes more unstable (Fig. 20) and the unstable layer rises (Fig. 19a), so both the intensification and the altitude of the peak intensity of the Hadley cells increase (Fig. 8).

Experiments SL7 and DL67 have clouds with the same cloud-top pressure, but different cloud-layer thicknesses, and exhibit quite different radiative cooling profiles (Fig. 19) and Hadley circulations (Fig. 8). Although the vertically integrated net radiation from the cloud layer is the same, representing the cloud with a single-model-layer eliminates by averaging the stronger heating and cooling features that the double-model-layer cloud is able to represent explicitly. The fact that the GISS GCM reacts dynamically to this smaller vertical-scale feature makes it significant for this model, if not realistic. No current GCM explicitly represents the profile of radiative heating within a cloud layer. Whether this is a deficiency depends on the vertical scale involved and whether that vertical scale should be represented, given the model horizontal resolution (see Lindzen and Fox-Rabinovitz 1989; Fox-Rabinovitz and Lindzen 1993). If dynamic modes with vertical scales less than about 1 km [the average layer thickness of clouds, (Wang 1997)] must be represented, then the dipole structure of radiative heating in a cloud layer may need to be explicitly represented in GCMs. This could be accomplished by splitting any cloud layer with a vertical extent $\geq$1 km into two explicit model layers for the radiation and dynamics subroutines or generally increasing the vertical resolution to resolve most cloud layers as two model layers. Surveys of cloud-layer thicknesses suggest that this would require vertical resolutions of 0.5 km (Poore et al. 1995; Wang and Rossow 1995; Wang 1997). Currently, most GCM cloud schemes only predict cloud-layer thicknesses by making separate predictions for each model layer (except for convective clouds); however, Del Genio et al. (1996) have developed a method for predicting cloud-layer thicknesses that are smaller than the model layers. The fact that such a difference in the model representation of even a single cloud layer causes significant changes in the model circulation calls attentions to the need for further investigation of GCM vertical resolution, especially involving clouds and radiation.

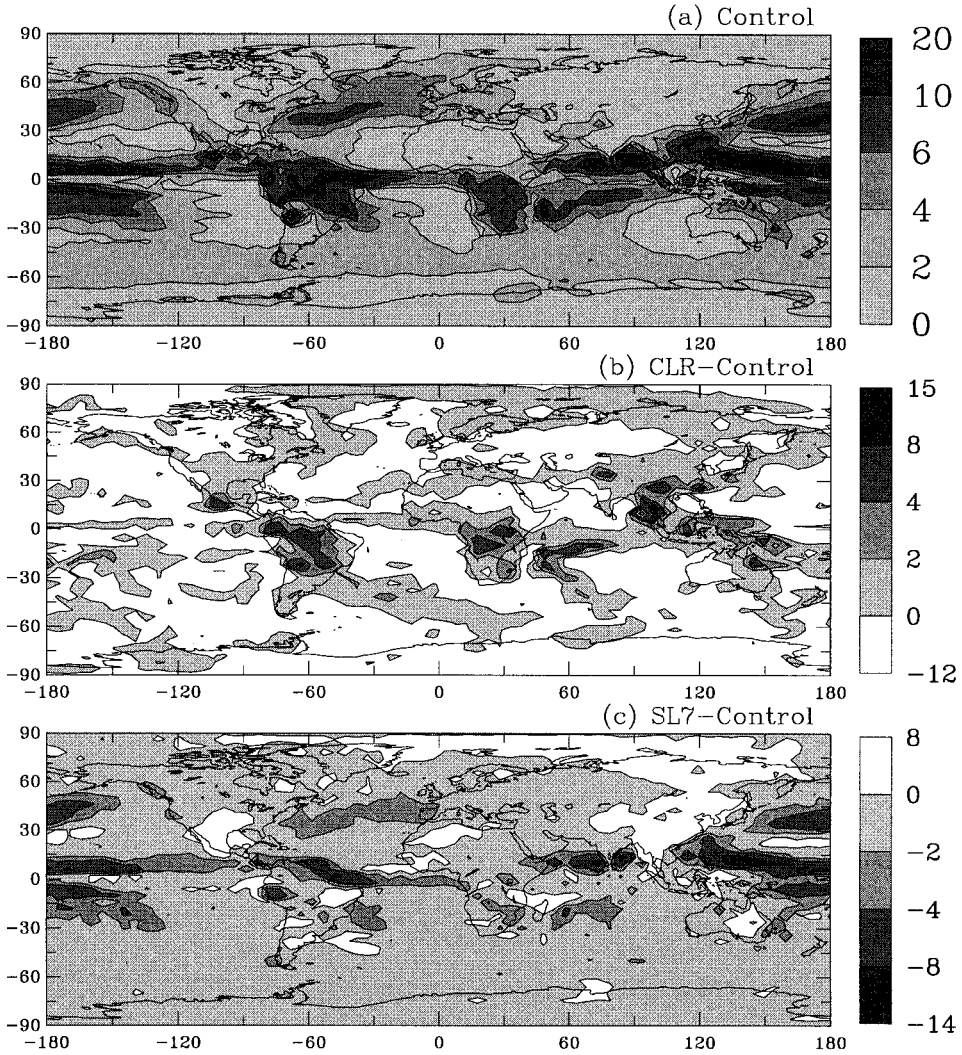

FIG. 14. (a) Global distribution of precipitation (mm day^{-1}) in the control run, (b) the difference between CLR and the control run, and (c) the difference between SL7 and the control run.

5. Discussion

Thirteen experiments have been performed with a new version of the GISS GCM to investigate the initial response of the large-scale circulation to imposed changes in its cloud vertical structure (CVS). We focus on the effects of changed CVS on the mean meridional circulation (MMC) and consider not only the direct changes of radiative cooling but also the feedback through induced changes in deep convection (latent heating). We also examine 1) the overall radiative effects of clouds on the model climate (clear versus cloudy skies), 2) the influence of the latitudinal and longitudinal variations of clouds (latitudinal and longitudinal variations versus globally uniform), and 3) the differences between the transient and equilibrium responses of the MMC. Several important points from the results are highlighted below.

a. Cloud-radiative effects

The effects of cloud changes on the earth and surface radiation budgets (ERB and SRB) are only indirectly related to the atmospheric circulation. For example, identical cloud-induced changes on ERB can produce drastically different changes in the vertical profiles of radiative fluxes, as happens in our experiments SL7 and DL67, where clouds have the same top pressure and total optical thickness. The different radiative cooling rate profiles (Fig. 19), however, cause noticeably different Hadley circulations (Fig. 8). Both Slingo and Slingo (1988) and Randall et al. (1989) also emphasized the importance to the atmospheric circulation of the vertical distribution of radiative fluxes within the atmosphere. Thus, we focus on the changes in radiative heating profiles within the atmosphere caused by changes in clouds, especially their vertical structure. To avoid

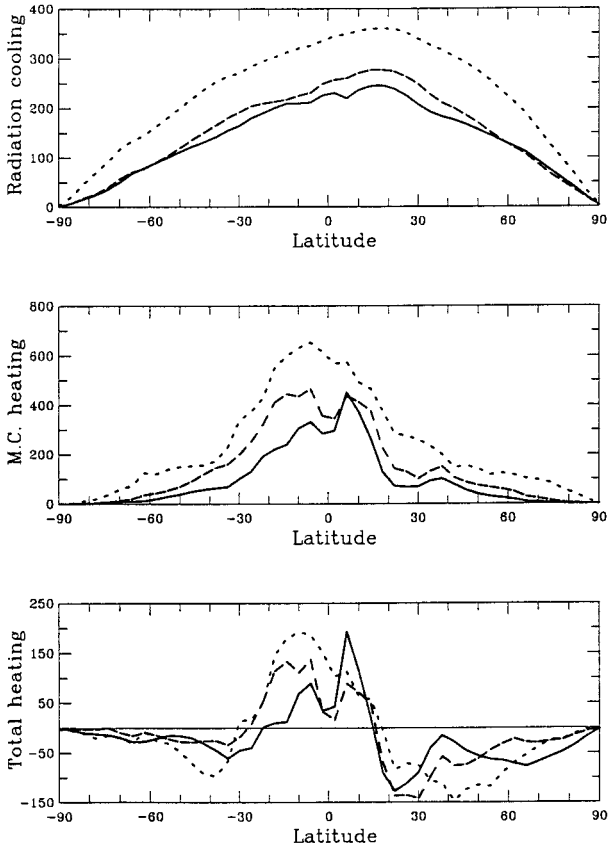

FIG. 15. (a) Vertically integrated radiative cooling, (b) moist convective heating, and (c) total diabatic heating as a function of latitude in the unit of 10^{13} W for the control run (solid line), CLR-E (short dashed line), and SL7-E (long dashed line).

confusion of terminology, we refer to changes of the radiative heating profiles induced by changes in clouds as the cloud radiative effect (CRE).

We evaluate the overall CRE and illustrate the complexity of determining the cloud effects with experiments CLR and CLR-E. The radiative and circulation changes induced by removing clouds in these two experiments are different because the atmospheric and surface properties (particularly temperature) are so different. In the transient experiment, atmospheric and surface temperatures are nearly the same as in the initial state, so that the CRE is the direct radiative effect of the cloud changes, together with the fast feedbacks, especially moist convection and the large-scale circulation. In the equilibrium experiment, the atmospheric and surface properties have changed dramatically from the initial state so that the CRE, if evaluated by comparing clear and cloudy radiative cooling rates (as commonly done), includes the response of the atmospheric and surface temperatures as well. Similarly, in the two single-layer experiments with clouds at the tropopause, SL7 and SL7-E, the CRE is very different when the atmospheric and surface temperature changes are included. Thus, the CLR results better represent the initial tendency produced by perturbing the clouds but not their ultimate feedback on the (model) climate.

b. Cloud effects on latent heating

When cloud changes induce perturbations in the radiative cooling rate profile, the effect on the atmospheric static stability also alters moist convective (latent) heat release. In our model, this feedback generally opposes

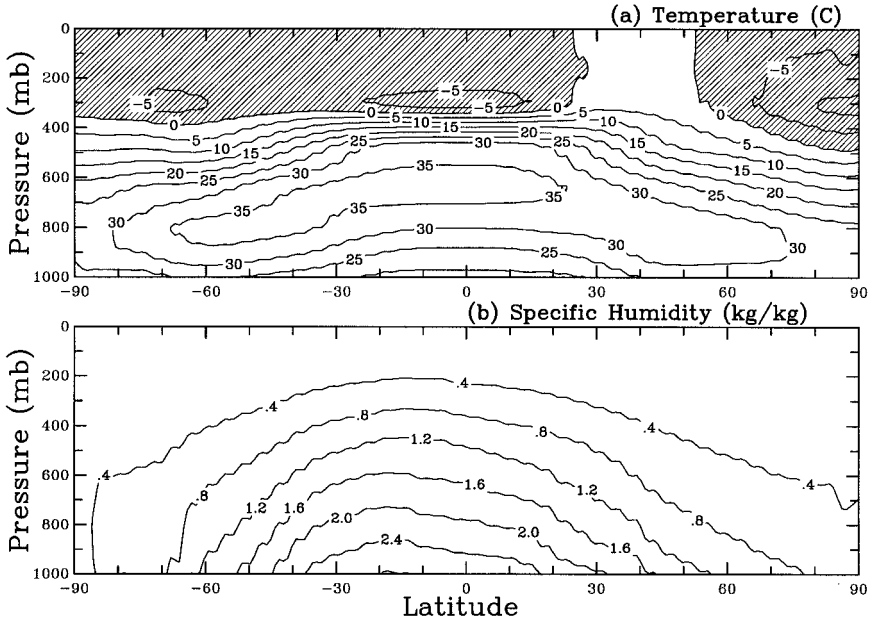

FIG. 16. The differences in (a) temperature (°C) and (b) specific humidity (kg kg^{-1}) between SL7-E and the control run.

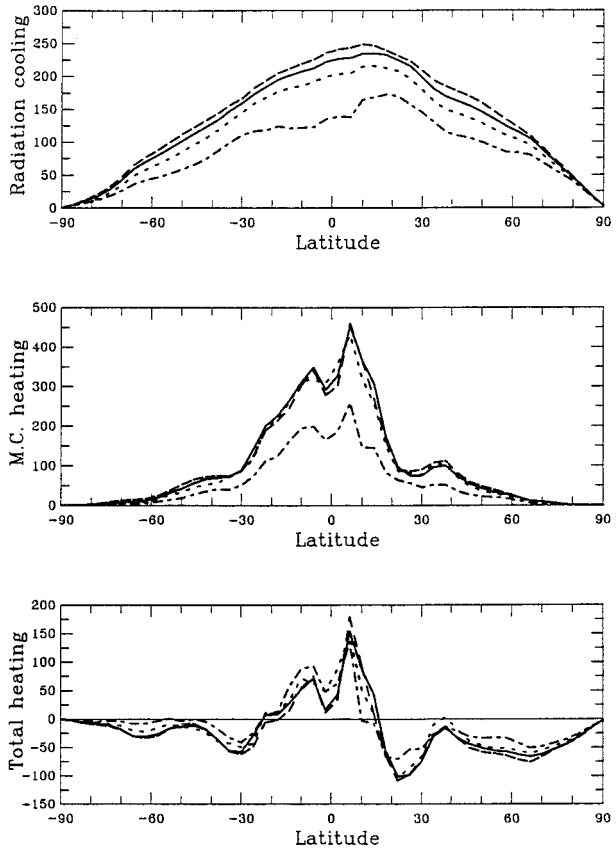

FIG. 17. (a) Vertically integrated radiative cooling, (b) moist convective heating, and (c) total diabatic heating as a function of latitude in the unit of 10^{13} W for the experiments with a single-model-layer cloud in layer 4 (SL4, solid line), 3 (SL3, long-dashed line), 5 (SL5, short-dashed line), and 7 (SL7, dot–dashed line).

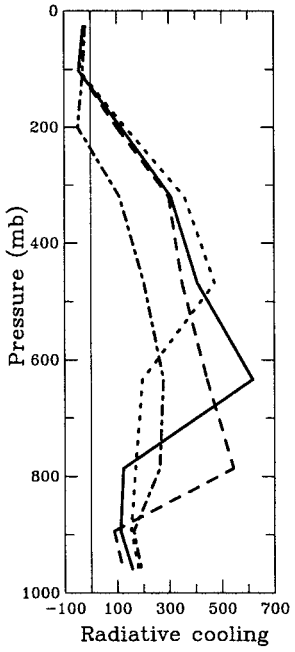

FIG. 18. Vertical profiles of integral of radiative cooling from 15°S to 15°N in the unit of 10^{13} W for the experiments with a single-model-layer cloud in layer 4 (SL4, solid line), 3 (SL3, long-dashed line), 5 (SL5, short-dashed line), and 7 (SL7, dot–dashed line).

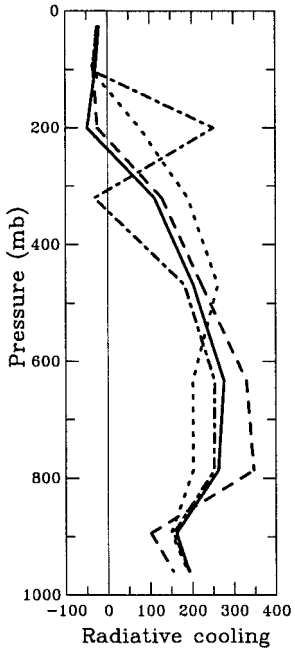

FIG. 19. Vertical profiles of integral of radiative cooling from 15°S to 15°N in the unit of 10^{13} W for SL7 with a single-model-layer cloud in layer 7 (SL7, solid line), and the experiments with two-layered clouds in layers 7/3 (DL37, long-dashed line), 7/5 (DL57, short-dashed line), and 7/6 (DL67, dot–dashed line).

the radiative perturbation, but does not always balance it locally or in detail because the two processes are not directly linked. In the clear-sky experiment, the transient response of the atmospheric thermal structure is small. Thus, removal of the clouds cools the upper atmosphere and warms the surface radiatively and the consequent destabilization increases convective heating in the Tropics, which happens to exceed the radiative cooling in magnitude. In the subtropics, removal of the clouds increases radiative cooling. Increased diabatic heating near the equator and increased cooling in the subtropics intensify the Hadley circulation. Thus, although the purely radiative effect of removing clouds would decrease the Hadley circulation, the operation of the other feedbacks, especially convection, changes the diabatic heating gradient and the resulting circulation response, in this model at least. Similarly in the other experiments, the responses of this model's Hadley circulation to the purely radiative perturbations induced by changes of CVS are significantly altered by induced changes of moist convection. Whether or not our particular GCM represents this coupling correctly, this link establishes

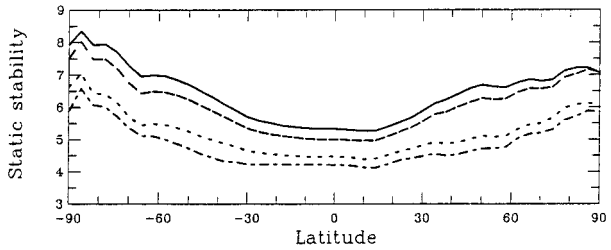

FIG. 20. Latitudinal variations of static stability (K km^{-1}) for SL7 (solid line), DL37 (long-dashed line), DL57 (short-dashed line), and DL67 (dot–dashed line).

the importance of CVS and its radiative consequences for a proper understanding of the climate.

c. Effects of spatial variations of cloud properties on the MMC

In all 13 experiments, total column cloud optical depth and cloud cover are still predicted by the GCM, so that their mean values and spatial distributions do not change from the control run except for feedbacks by the altered atmospheric properties and circulation. In 11 transient experiments, these changes were negligible and in the other two equilibrium experiments they were very small. The largest changes occurred in the moist convective cloud cover in the experiments with cloud-top pressures at 150 mb (SL7, DL37, DL57, and DL67): convective cloud cover decreased by about one-third, but this only represents a 6% change in total cloud cover. Therefore, we ignore changes in cloud cover and optical properties and focus on the changes of CVS and their spatial distribution.

In all 10 experiments in groups 2, 3, and 4 in Table 1, the Hadley circulation is suppressed relative to the control run (Table 2), because they lack the horizontal cloud height variations and have simpler CVS. When the model clouds are restricted to be single layered, introducing latitudinal variations in their heights, similar to those in the control run (ZMSL), strengthens the Hadley circulation, whereas introducing the longitudinal variations from the control run (GDSL) reduces the Hadley circulation. However, the effects of changes in the horizontal distribution of cloud heights are smaller than those produced by changing the vertical distribution, the CVS, away from a globally uniform, single-layered cloud. For example, inserting a cloud below layer 7 (DL37, DL57, and DL67) causes an increase in the vertically integrated peak intensities of the Hadley circulation in the NH by 18%, 33%, and 49%, respectively, compared with SL7, whereas introducing latitudinal cloud-height variations (ZMSL-SL4) only increases the peak intensity by 5% (Table 2). Changing latitudinal and longitudinal gradients of cloud properties also alters the eddy motions that are responsible for the thermally indirect Ferrel cells; but we focus on the Hadley circulation here.

Systematic changes in CVS alter the vertical gradient of radiative cooling, but the effect on the Hadley circulation is also altered by the radiation- and circulation-induced changes of deep convection. Moving a single-layer cloud either up or down from the control-climate-average cloud position in layer 4 suppresses the Hadley circulation further, more so as the cloud layer moves higher (see Fig. 7). Thus, for single-layered clouds with control run properties (optical thickness and area cover), the strongest Hadley circulation is produced by a cloud layer near the middle of the troposphere. Adding a second layer, even preserving the average height (experiment DL35), strengthens the Hadley circulation relative to a single-layer cloud. This suggests that the stronger Hadley circulation in the control run relative to that in SL4 can be approximately explained by the radiative effects of a significant fraction of multilayered clouds, together with the horizontal variations of cloud vertical distribution. In experiments with two-layered clouds having the uppermost cloud at the same location (DL37, DL57, and DL67), the Hadley circulation is stronger than with only a single-layer cloud (SL7). The fact that the largest difference appears for the experiment with one cloud layer represented by two model layers (DL67, Fig. 8) suggests that resolving the within-cloud radiative profile for deep cloud layers may be dynamically significant. Similar experiments with both layers at lower altitudes suggest a weaker dependence on vertical resolution. In experiments with two-layered clouds with the similar separation distances, but different mean heights (DL35 and DL57), the one with the lower cloud tops (DL35) has the stronger Hadley circulation (Table 2). The weaker and wider Hadley circulation in DL37 than in DL35 again demonstrates that as the height of uppermost cloud layer is elevated, and/or the gap between two-layered clouds is broadened, the intensity of Hadley circulation is suppressed, but its horizontal extension is increased. Therefore, all three parameters of the CVS, uppermost cloud-top height, the occurrence of multiple layers, and the separation distances between the layers, appear to have roughly equal significance in determining the Hadley circulation.

d. Significance of the results

The changes in cloud vertical structure imposed on the model in this study are idealized and much more extreme than would probably occur during a climate change. Moreover, the particular details and magnitudes of our model responses may be dependent on this model's convection and other schemes, particularly, on the order in which the physics subroutines are executed. For example, comparing the changes in precipitation in our CLR experiment, where surface temperatures change little, with the changes produced in the model of Slingo and Slingo (1988) by removing all cloud effects on longwave (LW) radiation shows that they are diametrically opposite; in their experiment, precipitation

is enhanced over the tropical areas where convection is concentrated, whereas in our experiment, it is suppressed. In their model, the cloud's LW radiative effect is a warming throughout the troposphere that intensifies the Hadley circulation and enhances the low-level convergence of moisture, thereby increasing convective activity and precipitation (despite stabilizing the upper-tropical troposphere). In our model (see section 4), the cloud radiative heating of the atmosphere first stabilizes the troposphere which, consequently, reduces convective activity and precipitation. Then the net effect of the radiative heating is offset by a decrease in latent heating resulting in a weakening of the Hadley circulation. These model differences highlight the need to understand the links among the large-scale dynamics, cloud-radiation interaction, and moist convection.

It is also plausible that the model's vertical resolution affects the details of this study. Whether the Hadley circulation is sensitive to increased vertical resolution depends on how the radiative profile varies with the model's vertical resolution and how the GCM responds to resultant perturbations in radiative profile. As pointed out in section 4d, the comparison of SL7 and DL67 implies that increasing our model's vertical resolution to 18 layers can result in significantly different Hadley circulations in our model because our model reacts dynamically to this smaller vertical scale feature.

Nevertheless, these experiments serve to highlight the role of CVS in affecting the atmospheric circulation and the role of feedbacks, particularly moist convection, in determining the response of the whole system. Although the magnitude of the changes in the Hadley circulation produced in our experiments is about the same as produced in this model when the CO_2 abundance is doubled (not shown), the changes in CVS that would occur during a climate change are likely to be much smaller. The similarity in magnitudes suggests that such CVS changes could constitute an important cloud feedback on climate change, in addition to others that have been studied. Comparing the transient and equilibrium experiments shows that the nature of such a feedback is ambiguous because the effect of the initial cloud-induced radiation changes can be altered by the subsequent response of the climate system. Moreover, the ''cloud radiative effect'' cannot usefully be considered separately from the role of clouds in the hydrological cycle, which is the other major component of the diabatic forcing of the atmospheric circulation.

e. Suggestions for model improvement

This study indicates some cloud parameters that must be observed and modeled accurately to obtain correct circulations: in addition to cloud-top and -base heights, the layer thicknesses and number of layers are also significant in determining the Hadley circulation. Changes in CVS affect the Hadley circulation by directly modifying the radiative cooling profile and indirectly modulating convective heating profile. Clouds with the same cloud-top pressure but different cloud-layer thicknesses (SL7 vs. DL67) produce quite different Hadley circulations (Fig. 8), indicating a sensitivity of the atmospheric circulation to details of the vertical heating/cooling profile at scales as small as ~2 km in this model. The dipole structure of radiative heating/cooling profile (base warming and top cooling) is also important for cloud formation and maintenance, such as for cirrus clouds (Starr and Cox 1985). Global and annual mean cloud-layer thickness is estimated to be 1.39 km (98 mb) (Wang 1997), with a mean separation distance for multilayered clouds of about 2.1 km (175 mb), suggesting model vertical resolutions may need to be at least 695 m (30–40 mb). However, it may be possible to parameterize both sublayer cloud thicknesses (e.g., Del Genio et al. 1996) and the more detailed radiative heating profile and its dynamic consequences. Note, we have not considered the additional effects on the radiative heating profile of vertical variations of optical properties within the cloud layer (e.g., Nicholls and Leighton 1986; Ackerman et al. 1988; Davies and Alves 1989; Matrosov et al. 1994). Consequently, observations of cloud vertical structures need a vertical resolution of at least 695 m (30 mb) to improve our understanding of these issues further.

Acknowledgments. It is a pleasure to thank Dr. A. D. Del Genio for many useful discussions and for providing computer time to run the experiments in the GISS GCM. Drs. M.-S. Yao and R. Ruedy helped in setting up the runs and answering questions regarding the GISS GCM. This research is supported by the NASA Global Observations and Radiation Program. J. Wang is grateful to Dr. J. Curry at the University of Colorado for support to finish writing this paper.

REFERENCES

Ackerman, T. P., K.-N. Liou, F. P. J. Valero, and L. Pfister, 1988: Heating rates in tropical anvils. *J. Atmos. Sci.,* **45,** 1606–1623.

Arking, A., 1991: The radiative effects of clouds and their impact on climate. *Bull. Amer. Meteor. Soc.,* **72,** 795–813.

Davies, R., and A. R. Alves, 1989: Flux divergence of thermal radiation within stratiform clouds. *J. Geophys. Res.,* **94,** 16 277–16 286.

Del Genio, A. D., 1996: TRMM: The tropical rainfall measuring mission. *Radiation and Water in the Climate System: Remote Measurements,* E. Raschke, Ed., NATO ASI Series, Springer-Verlag, 549–567.

——, and M.-S. Yao, 1993: Efficient cumulus parameterization for long-term climate studies: The GISS scheme. *The Representation of Cumulus Convection in Numerical Models, Meteor. Monogr.,* No. 46, Amer. Meteor. Soc., 181–184.

——, ——, W. Kovari, and K. K.-W. Lo, 1996: A prognostic cloud water parameterization for global climate models. *J. Climate,* **9,** 270–304.

Fox-Rabinovitz, M., and R. S. Lindzen, 1993: Numerical experiments on consistent horizontal and vertical resolution for atmospheric models and observing systems. *Mon. Wea. Rev.,* **121,** 264–271.

Fu, R., A. D. Del Genio, and W. B. Rossow, 1994: Influence of ocean

surface conditions on atmospheric vertical thermodynamic structure and deep convection. *J. Climate,* **7,** 1092–1108.
Gordon, A. L., 1982: *Southern Ocean Atlas.* Columbia University Press, 34 pp. and 248 plates.
Grotjahn, R., 1993: *Global Atmospheric Circulations*. Oxford University Press, 430 pp.
Hansen, J. E., G. Russell, D. Rind, P. Stone, A. Lacis, S. Lebedeff, R. Ruedy, and L. Travis, 1983: Efficient three-dimensional global models for climate studies: Models I and II. *Mon. Wea. Rev.,* **111,** 609–662.
——, A. Lacis, D. Rind, G. Russell, P. Stone, I. Fung, R. Ruedy, and J. Lerner, 1984: Climate Sensitivity: Analysis of feedback mechanisms. *Climate Processes and Climate Sensitivity*, *Geophys. Monogr.*, No. 29, Amer. Geophys. Union, 130–163.
——, I. Fung, A. Lacis, D. Rind, S. Lebedeff, R. Ruedy, and G. Gussell, 1988: Global climate changes as forecast by Goddard Institute for Space Studies three-dimensional model. *J. Geophys. Res.,* **93,** 9341–9364.
Hartmann, D. L., H. H. Hendon, and R. A. Houze, 1984: Some implications of the mesoscale circulations in tropical cloud clusters for large-scale dynamics and climate. *J. Atmos. Sci.,* **41,** 113–121.
Houze, R. A., 1982: Cloud clusters and large-scale vertical motions in the tropics. *J. Meteor. Soc. Japan,* **60,** 396–410.
Hunt, B. G., 1978: On the general circulation of the atmosphere without clouds. *Quart. J. Roy. Meteor. Soc.*, **104,** 91–102.
Hunt, G. E., V. Ramanathan, and R. M. Chervin, 1980: On the role of clouds in the general circulation of the atmosphere. *Quart. J. Roy. Meteor. Soc.,* **106,** 213–215.
Jin, Y., and W. B. Rossow, 1997: Detection of cirrus overlapping low-level clouds. *J. Geophys. Res.* **102,** 1727–1737.
Le Treut, H., and K. Laval, 1984: The importance of cloud-radiation interaction for the simulation of climate. *New Perspectives in Climate Modeling,* A. L. Berger, Ed., Elsevier, 199–221.
Liang, X.-Z., and W.-C. Wang, 1997: Cloud overlap effects on general circulation model climate simulations. *J. Geophys. Res.,* **102,** 11 039–11 047.
Lindzen, R. S., and M. Fox-Rabinovitz, 1989: Consistent vertical and horizontal resolution. *Mon. Wea. Rev.,* **117,** 2575–2583.
Machado, L. A. T., and W. B. Rossow, 1993: Structural characteristics and radiative properties of tropical cloud clusters. *Mon. Wea. Rev.,* **121,** 3234–3260.
Matrosov, S. Y., B. W. Orr, R. A. Kropfli, and J. B. Snider, 1994: Retrieval of vertical profiles of cirrus cloud microphysical parameters from Doppler radar and infrared radiometer measurements. *J. Appl. Meteor.,* **33,** 617–626.
Meleshko, V. P., and R. T. Wetherald, 1981: The effect of a geographical cloud distribution on climate: A numerical experiment with an atmospheric general circulation model. *J. Geophys. Res.*, **86,** 11 995–12 014.
Nicholls, S., and J. Leighton, 1986: An observational study of the structure of stratiform cloud sheets Part I: Structure. *Quart. J. Roy. Meteor. Soc.,* **112,** 431–460.
NOAA, 1974: User's guide to NODC data services. Environmental Data Service, 162 pp.
Poore, K., J. Wang, and W. B. Rossow, 1995: Cloud layer thickness from a combination of surface and upper-air observations. *J. Climate,* **8,** 550–568.
Ramaswamy, V., and V. Ramanathan, 1989: Solar absorption by cirrus clouds and the maintenance of the tropical upper troposphere thermal structure. *J. Atmos. Sci.,* **46,** 2293–2310.
Randall, D. A., Harshvardhan, D. A. Dazlich, and T. G. Corsetti, 1989: Interactions among radiation, convection, and large-scale dynamics in a general circulation model. *J. Atmos. Sci.,* **46,** 1943–1970.
Rind, D., and W. B. Rossow, 1984: The effects of physical processes on the Hadley circulation. *J. Atmos. Sci.,* **41,** 479–507.
Rossow, W. B., and A. A. Lacis, 1990: Global, seasonal cloud variations from satellite radiance measurements. Part II: Cloud properties and radiative effects. *J. Climate,* **3,** 1204–1253.
——, and Y.-C. Zhang, 1995: Calculation of surface and top-of-atmosphere radiative fluxes from physical quantities based on ISCCP datasets. Part II: Validation and first results. *J. Geophys. Res.,* **100,** 1167–1197.
Shukla, J., and Y. Sud, 1981: Effect of cloud-radiation feedback on the climate of a general circulation model. *J. Atmos. Sci.,* **38,** 2337–2353.
Slingo, A., and J. M. Slingo, 1988: The response of a general circulation model to cloud longwave radiative forcing. Part I: Introduction and initial experiments. *Quart. J. Roy. Meteor. Soc.,* **114,** 1027–1062.
——, and ——, 1991: The response of a general circulation model to cloud longwave radiative forcing. Part II: Further studies. *Quart. J. Roy. Meteor. Soc.,* **117,** 333–364.
Sohn, B.-J., and E. A. Smith, 1992a: The significance of cloud-radiative forcing to the general circulation on climate time scales—A satellite interpretation. *J. Atmos. Sci.,* **49,** 845–860.
——, and ——, 1992b: Global energy transports and the influence of clouds on transport requirements—A satellite analysis. *J. Climate,* **5,** 717–734.
——, and ——, 1992c: The modulation of the low-latitude radiation budget by cloud and surface forcing on interannual timescales. *J. Climate,* **5,** 831–846.
Starr, D. O., and S. K. Cox, 1985: Cirrus clouds. Part II: Numerical experiments on the formation and maintenance of cirrus. *J. Atmos. Sci.,* **42,** 2682–2694.
Stubenrauch, C. J., A. D. Del Genio, and W. B. Rossow, 1997: Implementation of subgrid cloud vertical structure inside a GCM and its effect on the radiation budget. *J. Climate,* **10,** 273–287.
Wang, J., 1997: Determination of cloud vertical structure from upper air observations and its effects on atmospheric circulation in a GCM. Ph.D. dissertation, Columbia University, 233 pp.
——, and W. B. Rossow, 1995: Determination of cloud vertical structure from upper-air observations. *J. Appl. Meteor.,* **34,** 2243–2258.
Warren, S. G., C. J. Hahn, and J. London, 1985: Simultaneous occurrence of different cloud types. *J. Climate Appl. Meteor.,* **24,** 658–667.
Webster, P. J., and G. L. Stephens, 1980: Tropical upper-tropospheric extended clouds: Inferences from winter MONEX. *J. Atmos. Sci.,* **37,** 1521–1541.
——, and ——, 1984: Cloud-radiation interaction and the climate problem. *The Global Climate,* J. Houghton, Ed., Cambridge University Press, 63–78.
Wielicki, B. A., R. D. Cess, M. D. King, D. A. Randall, and E. F. Harrison, 1995: Mission to Planet Earth: Role of clouds and radiation in climate. *Bull. Amer. Meteor. Soc.,* **76,** 2125–2153.
Zhang, Y.-C., and W. B. Rossow, 1997: Estimating meridional energy transports by the atmospheric and oceanic general circulations using boundary fluxes. *J. Climate,* **10,** 2358–2373.
——, ——, and A. A. Lacis, 1995: Calculation of surface and top-of-atmosphere radiative fluxes from physical quantities based on ISCCP datasets, Part I: Method and sensitivity to input data uncertainties. *J. Geophys. Res.,* **100,** 1149–1165.